

Self-Organized Formation of Quantum Dots: New Physics, New Chemistry, New Technology

Principal Investigators: Zhenyu Zhang,¹ John Wendelken,¹ Jian Shen¹

Collaborators: Kwonjae Yoo,^{1,2} Kalman Varga,¹ Frank Flack,³ Art Baddorf,¹ Max Lagally³

¹Condensed Matter Sciences Division

²The University of Tennessee

³The University of Wisconsin

Abstract

This LDRD initiative proposed to seize a unique opportunity to make major advances in nanoscale science, engineering, and technology by solving one persistent bottleneck problem of the field: mass production of quantum dots (QDs) with narrow size and uniform spatial distributions. The project was focused on demonstrating the wide applicability of a conceptually new synthesis method conceived at ORNL that is a refinement of a technique previously explored by Weaver.¹ The method, called buffer layer and charge-assisted growth (BLC), takes full advantage of simple physical laws (Coulomb repulsion) and surface growth kinetics to enable the formation of QDs of almost any material on any substrate. The discovery of the BLC method (US patent # 6,313,479) has offered unprecedented opportunities for fundamental and applied research in nanoscale science and technology. Using this method, we have achieved the fabrication of two important classes of QD arrays, magnetic (iron) QDs on either metal (copper) or semiconductor (silicon) substrate, and germanium QDs on silicon. In both cases, the QDs are in novel configurations characterised by the absence of a wetting layer. These configurations are most desirable for basic research as well as for potential applications in memory, optical, and nanoelectronic devices.

Introduction

This project has both theoretical and experimental components. On the theory side, we have simulated the growth patterns of QD arrays with the use of an inert gas buffer layer both without or with charging, demonstrating that the charging effect is dramatic. During the first two years, experimental work focused first on the details of the technique for growth of QDs via the buffer layer and charging approach. This work was performed initially at the University of Tennessee, but most work was subsequently performed at ORNL on two new experimental growth and analysis systems that were built during the first year. Initial efforts were highly successful with the achievement of QDs of iron on copper and silicon substrates with a reduced size and narrower size distribution than can be obtained without the charging step. Changing the buffer layer thickness, deposition rate and amount, and charging procedures were used to control the size and density of the QD distribution. Although none of these parameter variations led to the ideal ordering predicted by theory, some indication of ordering was indeed indicated in lines of QDs in localized regions.

Use of the novel buffer layer approach in the QD growth process was critical to two extended groups of experiments. In the first, the buffer-layer growth was a key element in a study of low-dimensional magnetism allowing the otherwise impossible growth of Fe QDs on Cu surfaces. In the second, the buffer-layer growth made possible the growth of Ge QDs on Si(100) without a wetting layer in defiance of the normal growth rules.

In addition to our focus on the growth of QDs, we have performed both experimental and theoretical studies of the stability of nanostructures after their creation. Scanning probe observations following

homoepitaxial growth of Cu nanostructures were followed by a theoretical analysis showing that the decay behavior is highly dependent on the crystalline orientation.

As a natural extension of the BLC idea, we have sought to find ways to achieve both spatial and size ordering without the use of an inert gas buffer layer. This effort has led to the discovery of the 2D magic clustering approach, leading to perfectly ordered metal magic clusters on a reconstructed surface of Si(111)-(7x7).

Technical Approach

A Novel Growth Concept

The purpose of this project is to develop a new and more general approach to the fabrication of self-organized QDs, (SOQDs). It can be used with virtually any combination of nanocluster material and substrate provided that an electric charge may be applied to the nanocluster material. The recipe is illustrated in Fig. 1 and contains the following steps: (1) condense and freeze a thick buffer layer of an inert gas and maintain the system at a temperature below the sublimation point of the buffer gas. (2) Deposit atoms of a metal or semiconductor on top of the buffer layer. These atoms will exhibit extremely high mobility on top of the buffer layer (compared to direct deposit without the buffer layer) and will diffuse to form a relatively low density of 3D clusters. (3) Charge the clusters by either photoionization or an electron beam. This electron charge interferes with the natural diffusion of the small clusters as the charged clusters begin to repel one another by Coulombic repulsion. In order to minimize the total electrostatic energy, the clusters will tend to develop a uniform spacing. (4) Continue the growth of the nanoclusters to the desired size. Each uniformly spaced nanoclusters acts as a nucleus for further growth and since each may collect arriving adatoms from approximately the same areas, they will grow to approximately the same size. (5) Raise the substrate temperature to remove the buffer layer. This provides a gentle landing of the nanocluster array with essentially the same spacing and size distribution as the original array on top of the buffer layer.

Theoretical Modeling

Before carrying out specific experiments, we have tested the BLC idea using kinetic Monte Carlo simulations. The main results are summarized in Fig. 2. Here the growth patterns were obtained under identical conditions (namely, the same growth temperature, same deposition rate, and same coverage), except for one aspect. On the left, the morphologies were obtained with the use of an inert gas buffer but without charging; on the right, charging was introduced simultaneously as the deposition proceeded. Whereas the island size and spatial distributions are random and dispersed in the left case, dramatically improved size and spatial distributions have been induced via charging.

In collaboration with an Italian group, we have also discovered a striking bimodal growth mode for QD formation in an entirely unexpected homoepitaxial system of Al(110), and the conceptual notions revealed in this study may significantly improve our current understanding of QD formation in heteroepitaxial systems as well.

Experimental

To test the feasibility and correctness of the above recipe in the laboratory after its theoretical verification required specially configured ultrahigh vacuum growth chambers. Requirements include a cryogenic sample stage on which the substrates can be cooled to 30 K or lower, a source of gaseous xenon, an evaporation source with low thermal output, a source of low energy (<5eV) electrons or a UV photon source, and finally, an in situ scanning probe to observe the QDs after growth. These requirements were

initially met using a scanning tunneling microscope (STM), at the University of Tennessee with custom-built sources from ORNL. Later, an existing room temperature vacuum STM at ORNL was equipped with a low-temperature growth chamber that allowed increased time and flexibility for the measurements. This same STM system was used to produce time-lapse movies of decaying nanostructures in order to better understand the forces affected their long-term stability. A new variable temperature vacuum atomic force microscopy (AFM) system was also developed in the first year that allowed the examination of the morphology of the insulating buffer layer before growth of the QDs. In studies of the magnetic properties low-dimensional magnetic nanostructures, additional growth techniques such as laser molecular beam epitaxy to produce 2D films and step-edge-assisted growth to produce 1D wires were used in conjunction with the buffer-layer-assisted growth technique. Utilization of these combined growth techniques allowed the growth of nanostructures of the same material in all these dimensional forms on a common substrate. Analysis was then performed in situ with the magneto-optical Kerr effect (MOKE). For optical characterization of semiconductor QDs, a protective capping layer of silicon was deposited over the QDs before shipment to collaborators at the University of Wisconsin who are well equipped for photoluminescence (PL) measurements in the infrared range.

Results and Accomplishments

Metallic QDs

To test the growth of metallic QDs utilizing the BLC approach, Fe dots were grown on xenon buffer layers on Cu(111), Cu(100), Si(111), and Si(100). The results were essentially the same in all cases as expected for this very general technique. Representative data is shown in Fig. 3 using the Fe/Cu(111) results as an example. A comparison of panels (a) and (b) show the effect of buffer layer thickness on the QD size distribution in the absence of the charging step in agreement with previously published results.² Panel (c) shows the effects of Coulomb repulsion resulting from the introduction of low energy electrons in the growth region during deposition of the Fe atoms on a buffer layer the same thickness as in panel (b). The average diameter is reduced from 7.5 nm to 2.2 nm, and the width is reduced from $\pm 50\%$ to $\pm 24\%$. Thus, two parts of the theoretical prediction concerning the size and the size distribution have been verified. Under some condition, it was also observed that the QDs will be organized into lines with highly uniform spacing, however, the ultimate goal of a uniformly organized array was not achieved.

In search of the factors inhibiting the spatially ordered formation of the QDs, experiments were performed in one of the new systems that is equipped with a variable temperature AFM. This allowed direct imaging of the surface of the solid xenon buffer layer at a temperature of 25 K. Our findings here may indicate the key problem. The surface of the xenon is found to be rough rather than smooth as expected. Very recent results suggest the possibility of improving the surface of the xenon by growing the xenon layers at a temperature just below the solidification temperature for xenon. Other potential problems for the ordering process include image charge when the substrate is metallic and turbulence when the buffer is removed.

Although we have not been able to form QDs that are highly ordered spatially yet, this approach offers the possibility of creating many useful structures for either experimental or applied purposes. One notable success has been in use of the buffer layer technique to create a controlled nanostructure of magnetic iron QDs in a study of low-dimensional magnetism. This is a remarkable success since Fe cannot be made into QDs on Cu(111) with any other growth methods. The magnetic characterization of the Fe dots reveals surprising magnetic stability at elevated temperatures (up to 140 K), which is now understood to be a result of large magnetic anisotropy and dipolar interaction between the dots. With the addition of buffer layer technique, we have now mastered a set of novel methods that enable us to grow 2D, 1D, and 0D magnetic nanostructures on a common template such as Cu(111) and W(110). Direct comparison of the

magnetic properties of these three structures has shown a surprising non-monotonic behavior as a function of the system dimensionality.

Silicon Compatible QDs

Another potentially very useful structure has been created using buffer-layer-assisted growth to create germanium QDs. Initial work has involved the growth of Ge QDs on xenon layers that are then deposited on Si(100) surfaces. For the first time, germanium QDs have been created without the usual wetting layer that characterizes the normal Stranski-Krastonow (SK) mode.³ In addition, the size distribution is one order of magnitude smaller than can be obtained with conventional growth techniques. This smaller size and lack of a wetting layer can result in improved quantum confinement with enhanced optical properties. Figure 4a shows an STM image of the Ge QDs following the deposition of 0.5 monolayer (ML) equivalent of Ge atoms on a 6 ML xenon buffer layer without electron charging. Figure 5 shows the measured width and height distributions of this sample with an average width of ~3 nm and an average height of ~0.6 nm. Panels (b) and (c) in Fig. 4 reveal an unexpected problem that was encountered as the buffer layer thickness was increased. Aggregation of the QDs into chains developed for buffer layer thicknesses of 10 ML and above with an extreme aggregation effect for a buffer layer of 40 ML. A similar behavior was recently reported for Au clusters on graphite grown with much thicker buffer layers.⁴ This inhibits our desired ability to control the size of the QDs. Electron charging may reduce the aggregation, but it is also expected to reduce the size of the QDs as was observed with the Fe case.

The optical properties of the Ge QD structures produced in this project have been characterized in the infrared range by PL measurements at the University of Wisconsin. Figure 6 shows the spectra obtained for both a single-layer structure and a three-layer structure. For the three-layer structure, spacer layers of *p*-doped Si are grown on top of the QDs at room temperature, then the system is cooled again for the buffer-layer-growth process for each layer. The spectra obtained for both structures have two principal peaks at the same energies. This is remarkable in view of recent results obtained for a two-layer QD structure of SK grown QDs in which the spectrum shows a blue shift and an additional peak resulting from the second layer.⁵ This layer dependence stems from the increased stress at the growth front of the second layer that results in increased intermixing of the Si with the Ge, a problem which is clearly not present with the buffer-layer-assisted growth. The observed spectrum with two principal peaks is not consistent with the published⁶ single-layer SK QD spectra that show only one peak. In the conventional SK growth method, the QDs possess a highly strained interface with the surrounding silicon resulting in a neighboring confinement structure⁷ and a type II band alignment with transitions from electrons trapped in the interface to holes in the germanium QDs. The low-temperature deposition of the silicon used in the present work to avoid alloying of the Ge with the Si results in QDs surrounded by amorphous Si, and little interface strain. An observed independence of the spectrum with increasing power, Fig. 7, is not consistent with the blueshift expected with a type II band alignment. The observed spectrum is more similar to the spectra reported for Ge QDs grown on SiO₂, where the reduced strain results in a type I band alignment⁸ and two PL peaks associated with a no-phonon direct transition and its phonon replica. However, the observed downshift in energy with increasing temperature, Fig. 8, is not consistent with a type I band alignment. All of the observations are consistent with a defect-associated origin⁹ in terms of peak energies and power and temperature dependences. Thus, a future direction will be to deposit the Ge QDs on a SiO₂ surface to allow annealing and crystallization of the QDs.

Self-assembly of Perfectly Ordered 2D Magic Nanocluster Arrays

As a natural extension of the BLC idea, we have sought to find ways to achieve both spatial and size ordering without the use of an inert gas buffer layer. This effort has resulted in the discovery of the 2D magic clustering approach, leading to perfectly ordered metal magic clusters on a reconstructed surface of Si(111)-(7x7).

Fundamental Physics of QD Growth and Stability

In addition to the growth of QDs, fundamental studies have been carried out to examine the stability of QDs and nanostructures after growth. In the experimental part of this study, nanostructures of Cu on Cu(100) and Cu(111) were created and then observed by STM to see their behavior with time at room temperature. The decay behavior on the two structures was quite different with a uniform decay at all levels occurring on the Cu(111) surface, while on the Cu(100) surface, the decay occurred from the bottom of a mound first. In both cases, the decay process occurred primarily through an avalanche process when one atomic height step approached a step of a supporting layer below. The orientation of the supporting step edge was very important in the (100) case, while orientation was insignificant in the (111) case. This observation has been explained in a model study that showed that all the observed qualitative behavior could be determined by whether the system observed decayed by an “any site decay” mechanism or by a “selective site decay” mechanism.

Summary and Conclusions

In summary, a novel and very general technique for the growth of QDs of any material on any substrate has been extended by introduction of a charging step to the buffer-layer-growth process. The buffer-layer-growth technique has been employed as a key element in the study of nanoscale magnetism, permitting the growth of 0D as well as 2D and 1D magnetic nanostructures of the same material on a single type of substrate. The stability of nanostructures after creation has been experimentally explored by direct scanning probe observation and theoretical analysis has revealed a distinct difference in fundamental decay behavior dependent on crystallographic orientation of the substrate.

These research findings have resulted in 10 invited talks at major scientific meetings, including 2 keynote speech invitations. About 15 contributed talks have also been presented/scheduled.

References

- ¹J. H. Weaver and G. D. Waddill, “Cluster assembly of interfaces: nanoscale engineering,” *Science* **251**, 1444 (1991).
- ²S. J. Chey and J. H. Weaver, “Self-assembly of multilayer arrays from Ag nanoclusters delivered to Ag(111) by soft landing,” *Surf. Sci.* **419**, L100 (1998).
- ³J. Wan, G. L. Jin, Z. M. Jiang, Y. H. Luo, J. L. Liu, and K. L. Wang, “Band alignments and photon-induced carrier transfer from wetting layers to Ge islands grown on Si(001),” *Appl. Phys. Lett.* **78**, 1763 (2001).
- ⁴Christina Haley and J. H. Weaver, “Buffer-layer-assisted nanostructure growth via two-dimensional cluster-cluster aggregation,” *Surf. Sci.* **518**, 243 (2002).
- ⁵M. Larsson, A. Elfving, P.-O. Holtz, G. Hansson, and W.-X. Ni, “Photoluminescence study of Si/Ge quantum dots,” NANO-7 and ECOSS-21, Malmo, Sweden (2002).
- ⁶S. Fukatsu, H. Sunamura, Y. Shiraki, and S. Komiyama, “Phononless radiative recombination of indirect excitons in a Si/Ge type-II quantum dot,” *Appl. Phys. Lett.* **71**, 258 (1997).
- ⁷N. Usami, M. Miura, H. Sunamura, and Y. Shiraki, “Photoluminescence from pure-Ge/pure-Si neighboring confinement structure,” *J. Vac. Sci. Technol. B* **16**, 1710 (1998).

⁸A. Shklyaev and M. Ichikawa, "Effect of interfaces on quantum confinement in Ge dots grown on Si surfaces with a SiO₂ coverage," *Surf. Sci.* **514**, 19 (2002).

⁹S. Fukatsu, Y. Mera, M. Inoue, K. Maeda, H. Akiyama and H. Sakaki, "Time-resolved D-band luminescence in strain-relieved SiGe/Si," *Appl. Phys. Lett.* **68**, 1889 (1996).

Publications Derived from this Project

M. C. Chang and Z. Y. Zhang, "Self-organized formation of quantum dots assisted by an inert gas buffer layer and charging," (preprint).

J. Shen and J. Kirschner "Tailoring magnetism in artificially structured materials: the new frontier," *Surf. Sci.* **500**, 300 (2002).

J. Shen, J. P. Pierce, E. W. Plummer, and J. Kirschner, "The effect of spatial confinement on magnetism: films, stripes, and dots of Fe on Cu(111)," *J. Phys: Condensed Matter* (**review article**, in press).

Zheng Gai, Biao Wu, J. P. Pierce, G. A. Farnan, D. J. Shu, M. Wang, Zhenyu Zhang, and J. Shen, "Self-assembly of nanometer-scale magnetic dots with narrow size distributions on an insulating substrate," *Phys. Rev. Lett.* **89**, 235502 (2002).

Zheng Gai, G. A. Farnan, J. P. Pierce, and J. Shen, "Growth of low-dimensional magnetic nanostructures on an insulator," *Appl. Phys. Lett.* **81**, 742 (2002).

Jin-Feng Jia, Xi Liu, Jun-Zhong Wang, Jian-Long Li, X. S. Wang, Qi-Kun Xue, Zhi-Qiang Li, Zhenyu Zhang, and S. B. Zhang, "Fabrication and structural analysis of Al, Ga, and In nanocluster crystals," *Phys. Rev. B* **66**, 165412 (2002).

Yugui Yao, Ph. Ebert, Maozhi Li, Zhenyu Zhang, and E. G. Wang, "Decay characteristics of two-dimensional islands on strongly anisotropic surfaces," *Phys. Rev. B* **66**, 041407 (2002).

Jian-Long Li, Jin-Feng Jia, Xue-Jin Liang, Xi Liu, Jun-Zhong Wang, Qi-Kun Xue, Zhi-Qiang Li, John S. Tse, Zhenyu Zhang, and S. B. Zhang, "Spontaneous assembly of perfectly ordered identical-size nanocluster arrays," *Phys. Rev. Lett.* **88**, 066101 (2002).

Z. Gai, G. A. Farnan, J. P. Pierce, and J. Shen, "Growth of low-dimensional magnetic nanostructures on an insulator," *Appl. Phys. Lett.* **81**, 742 (2002).

J. Shen and J. Kirschner, "Tailoring magnetism in artificially structured materials: the new frontier," *Surf. Sci.* **500**, 300 (2002) (review article).

E. G. Wang, B. G. Liu, J. Wu, M. Z. Li, Y. G. Yao, W. G. Zhu, J. X. Zhong, J. F. Wendelken, Q. Niu, and Z. Y. Zhang, "Novel formation and decay mechanisms of nanostructures on the surface," *Chinese Phys.* **10**, S144 (2001).

Jing Wu, Enge Wang, Kalman Varga, Banggui Liu, S. T. Pantelides, and Zhenyu Zhang, "Island shape selection in Pt(111) submonolayer homoepitaxy with or without CO as an adsorbate," *Phys. Rev. Lett.* **89**, 146103 (2002).

A. G. Naumovets and Z. Y. Zhang, "Fidgety particles on surfaces: how do they jump, walk, group, and settle in virgin areas?" *Surf. Sci.* **500**, 414 (2002) (invited review).

Maozhi Li, Enge Wang, Yugui Yao, Shudun Liu, and Zhenyu Zhang, "Dynamical scaling of island-size distribution in anisotropic submonolayer epitaxial growth," *Phys. Rev. Lett.* (submitted).

K. Varga, L. G. Wang, S. Pantelides, and Z. Y. Zhang, "Critical layer thickness in Stranski-Krastanow growth of Ge on Si(001)," *Phys. Rev. Lett.* (submitted).

M. Z. Li, J. F. Wendelken, B. G. Liu, E. G. Wang, and Z. Y. Zhang, "Decay characteristics of surface mounds with contrasting interlayer mass transport channels," *Phys. Rev. Lett.* **86**, 2345 (2001).

W. W. Pai, J. F. Wendelken, C. R. Stoldt, P. A. Thiel, J. W. Evans, and D. J. Liu, "Evolution of two-dimensional wormlike nanostructures on metal surfaces," *Phys. Rev. Lett.* **86**, 3088 (2001).

F. Buatier de Mongeot, R. Buzio, A. Molle, C. Boragno, U. Valbusa, W. G. Zhu, E. G. Wang, and Z. Y. Zhang, "Nanocrystal formation via bimodal growth in Al(110) homoepitaxy: true upward diffusion and the role of surface 'Kinetic Traps'," *Nature* (submitted, under review).

Intellectual Property Derived from this Project

Z. Y. Zhang, J. F. Wendelken, M. C. Chang, and W. W. Pai, "Self-Organized Formation of Quantum Dots of a Material on a Substrate" (concerning the product, awarded 2001, US patent # 6,313,479).

Z. Y. Zhang, J. F. Wendelken, M. C. Chang, and W. W. Pai, "Self-Organized Formation of Quantum Dots of Almost Any Material on Any Substrate" (concerning the principal, pending).

Figure Captions

Fig. 1. Schematic of new growth process using buffer layer and charging technique. The steps in the growth process are illustrated sequentially from left to right.

Fig. 2. Theoretical prediction of effect of Coulomb repulsion when incorporated in buffer-layer growth process. Panel on left shows predicted distribution of QDs using standard buffer-layer-assisted growth and panel on right shows the expected QD distribution under the same growth conditions, but with the addition of electron charging in the early growth process.

Fig. 3. Experimental STM data for growth of Fe QDs on Cu(111) surface using buffer-layer-assisted growth: (a) standard buffer-layer-assisted growth with a 6 ML Xe buffer, (b) standard buffer-layer-assisted growth with a 40 ML Xe buffer, (c) buffer-layer growth with electron charging and with 40 ML Xe buffer. The quantity of Fe deposited is the same in all cases. The corresponding size distributions are shown below each STM image. Image sizes are 200 x 200 nm².

Fig. 4. Growth of Ge QDs as a function of buffer layer thickness: (a) 6 ML Xe buffer, (b) 10 ML Xe buffer, and (c) 40 ML Xe buffer. All STM images are obtained at room temperature with a Si(100) substrate after removal of the buffer layer. Image sizes are 100 x 100 nm².

Fig. 5. Typical size distribution for Ge QDs deposited on Si(100) via buffer-layer-assisted growth. No charging is used in this case.

Fig. 6. PL spectra obtained for single layer and triple layer Ge QD structures grown using buffer-layer-assisted growth process. Schematics of the examined samples are shown at the left of the corresponding PL spectra. Only the peak ratios change as a function of layer number indicating that every layer has the same purity. The intensities are in arbitrary units and the energy scale is in eV.

Fig. 7. Dependence of primary peaks on incident power in PL spectra obtained from Ge QD structures.

Fig. 8. Temperature dependence of primary peaks in PL spectra obtained from Ge QD structures.

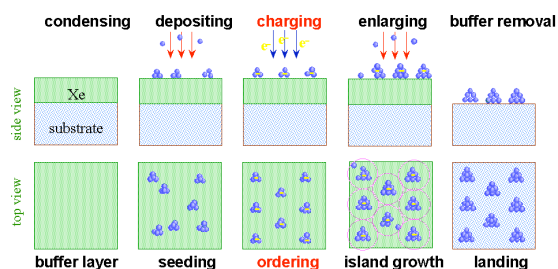


Fig. 1. Schematic of new growth process using buffer layer and charging technique. The steps in the growth process are illustrated sequentially from left to right.

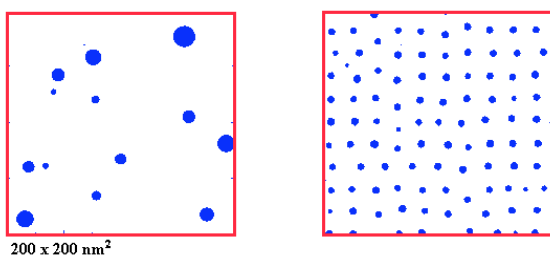


Fig. 2. Theoretical prediction of effect of Coulomb repulsion when incorporated in buffer-layer growth process. Panel on left shows predicted distribution of QDs using standard buffer-layer-assisted growth and panel on right shows the expected QD distribution under the same growth conditions, but with the addition of electron charging in the early growth process.

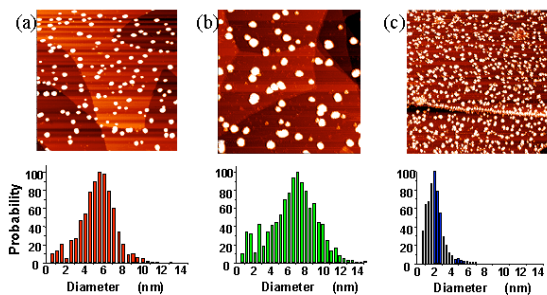


Fig. 3. Experimental STM data for growth of Fe QDs on Cu(111) surface using buffer-layer-assisted growth: (a) standard buffer-layer-assisted growth with a 6 ML Xe buffer, (b) standard buffer-layer-assisted growth with a 40 ML Xe buffer, (c) buffer-layer growth with electron charging and with 40 ML Xe buffer. The quantity of Fe deposited is the same in all cases. The corresponding size distributions are shown below each STM image. Image sizes are $200 \times 200 \text{ nm}^2$.

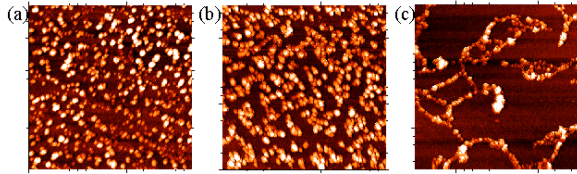


Fig. 4. Growth of Ge QDs as a function of buffer layer thickness: (a) 6 ML Xe buffer, (b) 10 ML Xe buffer, and (c) 40 ML Xe buffer. All STM images are obtained at room temperature with a Si(100) substrate after removal of the buffer layer. Image sizes are $100 \times 100 \text{ nm}^2$.

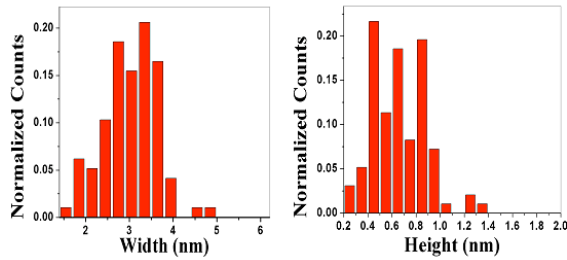


Fig. 5. Typical size distribution for Ge QDs deposited on Si(100) via buffer-layer-assisted growth. No charging is used in this case.

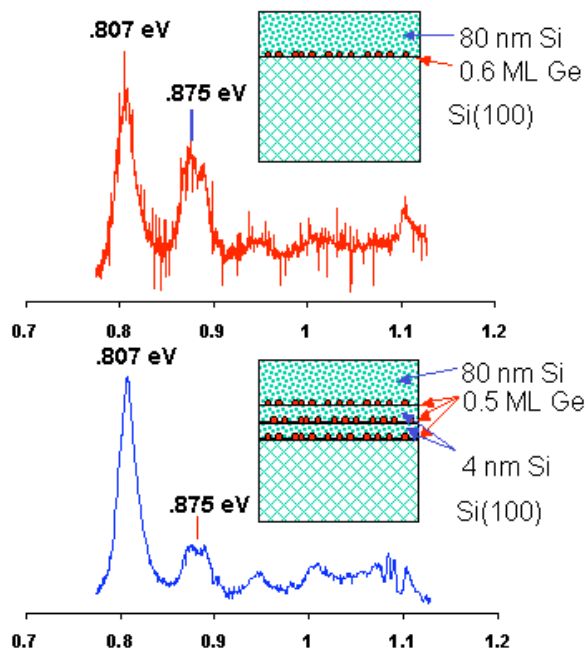


Fig. 6. PL spectra obtained for single layer and triple layer Ge QD structures grown using buffer-layer-assisted growth process. Schematics of the examined samples are shown at the left of the corresponding PL spectra. Only the peak ratios change as a function of layer number indicating that every layer has the same purity. The intensities are in arbitrary units and the energy scale is in eV.

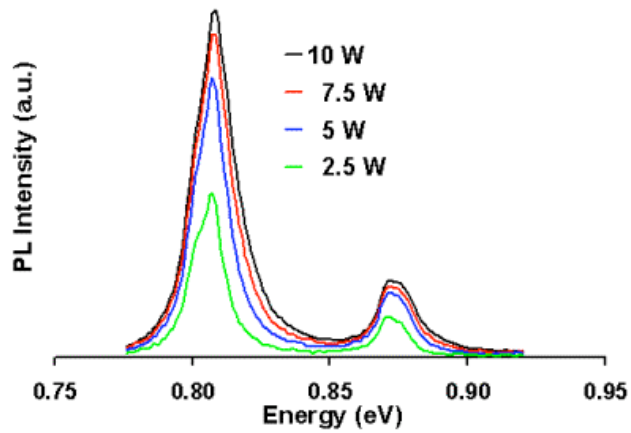


Fig. 7. Dependence of primary peaks on incident power in PL spectra obtained from Ge QD structures.

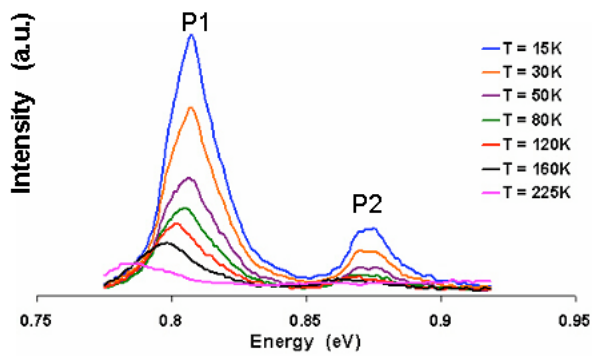


Fig. 8. Temperature dependence of primary peaks in PL spectra obtained from Ge QD structures.